1521-0103/361/1/140–150$25.00
THE JOURNAL OF PHARMACOLOGY AND EXPERIMENTAL THERAPEUTICS

http://dx.doi.org/10.1124/jpet.116.237701
J Pharmacol Exp Ther 361:140–150, April 2017

Overlapping and Divergent Actions of Structurally Distinct Histone Deacetylase Inhibitors in Cardiac Fibroblasts[S]

Katherine B. Schuetze, Matthew S. Stratton, Weston W. Blakeslee, Michael F. Wempe, Florence F. Wagner, Edward B. Holson, Yin-Ming Kuo, Andrew J. Andrews, Tonya M. Gilbert, Jacob M. Hooker, and Timothy A. McKinsey

Division of Cardiology and Consortium for Fibrosis Research and Translation, Department of Medicine, University of Colorado Anschutz Medical Campus, Aurora, Colorado (K.B.S., M.S.S., W.W.B., T.A.M.); Department of Pharmaceutical Sciences, Skaggs School of Pharmacy and Pharmaceutical, Sciences, University of Colorado Denver, Aurora, Colorado (M.F.W.); Stanley Center for Psychiatric Research, Broad Institute of Massachusetts Institute of Technology and Harvard, Cambridge, Massachusetts (F.F.W., E.B.H.); Department of Cancer Biology, Fox Chase Cancer Center, Philadelphia, Pennsylvania (Y.-M.K., A.J.A.); and Athinoula A. Martinos Center for Biomedical Imaging, Department of Radiology, Massachusetts General Hospital, Harvard Medical School, Charlestown, Massachusetts (T.M.G., J.M.H.)

Received September 10, 2016; accepted January 23, 2017

ABSTRACT

Inhibitors of zinc-dependent histone deacetylases (HDACs) profoundly affect cellular function by altering gene expression via changes in nucleosomal histone tail acetylation. Historically, investigators have employed pan-HDAC inhibitors, such as the hydroxamate trichostatin A (TSA), which simultaneously targets members of each of the three zinc-dependent HDAC classes (classes I, II, and IV). More recently, class- and isoform-selective HDAC inhibitors have been developed, providing invaluable chemical biology probes for dissecting the roles of distinct HDACs in the control of various physiologic and pathophysiological processes. For example, the benzamide class I HDAC-selective inhibitor, MGCD0103 [*N*-(2-aminophenyl)-4-[[(4-pyridin-3-ylpyrimidin-2-yl)amino]methyl] benzamide], was shown to block cardiac fibrosis, a process involving excess extracellular matrix deposition, which often results in heart dysfunction. Here, we compare the mechanisms of action of structurally distinct HDAC inhibitors in isolated primary cardiac fibroblasts, which are the major extracellular matrix–producing cells of the heart. TSA, MGCD0103, and the cyclic peptide class I HDAC inhibitor, apicidin, exhibited a common ability to enhance histone acetylation, and all potently blocked cardiac fibroblast cell cycle progression. In contrast, MGCD0103, but not TSA or apicidin, paradoxically increased expression of a subset of fibrosis-associated genes. Using the cellular thermal shift assay, we provide evidence that the divergent effects of HDAC inhibitors on cardiac fibroblast gene expression relate to differential engagement of HDAC1- and HDAC2-containing complexes. These findings illustrate the importance of employing multiple compounds when pharmacologically assessing HDAC function in a cellular context and during HDAC inhibitor drug development.

Introduction

Histone deacetylases (HDACs) are a family of 18 enzymes categorized into four classes. Class I, II, and IV HDACs are zinc dependent, and class III HDACs/sirtuins are NAD^+ dependent (Gregoretti et al., 2004). Canonically, HDACs function to regulate gene expression by removing acetyl groups from lysine residues within nucleosomal histone tails. Noncanonically, HDACs also catalyze the deacetylation of nonhistone targets, including a wide variety of both nuclear and cytoplasmic proteins, which significantly affects diverse biologic processes via alterations in protein stability, function, and cell signaling (Choudhary et al., 2009, 2014; Lundby et al., 2012). As would be expected with this broad range of biologic impact, HDACs have been implicated in numerous disease processes, including hematologic neoplasms, heart failure,

This research was supported by the National Institutes of Health National Heart, Lung and Blood Institute [Grants R01HL116848 and R01HL127240 (to T.A.M.), T32 Training Grants 5T32HL007822-12 (to K.B.S.) and 5T32HL007822 (to M.S.S.), and F32 Fellowship F32HL126354 (to M.S.S.)]; the National Institutes of Health National Institute on Aging [Grant R21AG043822 (to T.A.M.)]; and the American Heart Association [Grant 16SFRN31400013 (to T.A.M.)].

K.B.S. and M.S.S. contributed equally to this work.

dx.doi.org/10.1124/jpet.116.237701.

[S] This article has supplemental material available at jpet.aspetjournals.org.

ABBREVIATIONS: 4SC-202, (*E*)-*N*-(2-aminophenyl)-3-[1-[4-(1-methylpyrazol-4-yl)phenyl]sulfonylpyrrol-3-yl]prop-2-enamide; AMVF, adult mouse ventricular fibroblast; ARVF, adult rat ventricular fibroblast; BRD3308, 4-acetamido-*N*-(2-amino-4-fluorophenyl)benzamide; CETSA, cellular thermal shift assay; CHX, cycloheximide; CI-994, 4-acetamido-*N*-(2-aminophenyl)benzamide; DMEM, Dulbecco's modified Eagle's medium; DMSO, dimethylsulfoxide; ECM, extracellular matrix; FBS, fetal bovine serum; FDA, U.S. Food and Drug Administration; HDAC, histone deacetylase; LBH589, (*E*)-*N*-hydroxy-3-[4-[[2-(2-methyl-1*H*-indol-3-yl)ethylamino]methyl]phenyl]prop-2-enamide; MGCD0103, *N*-(2-aminophenyl)-4-[[(4-pyridin-3-ylpyrimidin-2-yl)amino]methyl] benzamide; MMP, matrix metalloprotease; MS-275, pyridin-3-ylmethyl-*N*-[[4-[(2-aminophenyl)carbamoyl]phenyl]methyl]carbamate; NRVF, neonatal rat ventricular fibroblast; NRVM, neonatal rat ventricular myocyte; PAI-1, plasminogen activator inhibitor type 1; PBS, phosphate-buffered saline; PCR, polymerase chain reaction; PEI, polyethyleneimine; PSG, penicillin, streptomycin, and L-glutamine; PXD101, (*E*)-*N*-hydroxy-3-[3-(phenylsulfamoyl)phenyl]prop-2-enamide; qPCR, quantitative polymerase chain reaction; TGF, transforming growth factor; TSA, trichostatin A.

neurodegenerative diseases, atherosclerosis, bone health, and fibrosis.

Given the involvement of HDACs in the pathogenesis of various diseases, there has been intense interest in HDAC inhibitor–based therapeutic approaches (Wagner et al., 2010; McKinsey, 2012). Indeed, four HDAC inhibitors are approved by the U.S. Food and Drug Administration (FDA) for the treatment of cancer, and a multitude of clinical trials are ongoing to test for efficacy of HDAC inhibitors in additional oncology indications as well as for nononcologic diseases (Fenichel, 2015; Mottamal et al., 2015). Generally, HDAC inhibitors are categorized into four groups based on chemical structure: hydroxamic acids, cyclic peptides, short-chain fatty acids, and ortho-amino anilides. HDAC inhibitors typically possess a conventional tripartite structure, with a zinc-binding group that chelates the zinc ion in the deacetylase catalytic site, a linker, and a surface recognition domain that interacts with residues near the entrance to the active site (Finnin et al., 1999). Within the chemical classes of HDAC inhibitors, there are both broad-spectrum, pan-HDAC inhibitors, as well as HDAC inhibitors that are selective for particular HDAC classes or isoforms (Wagner et al., 2013). However, it should be emphasized that the use of "pan" and "isoform-selective" to describe HDAC inhibitors is an oversimplification. For example, although hydroxamates exhibit broad-spectrum HDAC inhibitory activity in vitro (Bradner et al., 2010), chemoproteomic studies have demonstrated that these compounds engage only a subset of zinc-dependent HDACs in the cellular context (Bantscheff et al., 2011).

Of the four FDA-approved HDAC inhibitors, all are pan-inhibitors, three are hydroxamates (vorinostat [suberoylanilide hydroxamic acid], belinostat [PXD101, (E)-N-hydroxy-3-[3-(**N**-phenylsulfamoyl)phenyl]prop-2-enamide, and panobinostat [LBH589, (*E*)-*N*-hydroxy-3-[4-[[2-(2-methyl-1*H*-indol-3-yl) ethylamino]methyl]phenyl]prop-2-enamide]), and one is a cyclic peptide (romidepsin). Ortho-amino anilides, including the benzamide class I HDAC inhibitors entinostat [MS-275; pyridin-3-ylmethyl-*N*-[[4-[(2-aminophenyl)carbamoyl]phenyl] methyl]carbamate] and mocetinostat [MGCD0103, [*N*-(2-aminophenyl)-4-[[(4-pyridin-3-ylpyrimidin-2-yl)amino]methyl] benzamide], and 4SC-202 [(*E*)-*N*-(2-aminophenyl)-3-[1-[4-(1-methylpyrazol-4-yl)phenyl]sulfonylpyrrol-3-yl]prop-2-enamide], which is not a benzamide, are currently being evaluated in multiple clinical trials, and the short-chain fatty acid, valproate, has been used to treat neurologic disorders for decades (Terbach and Williams, 2009). It should be noted, however, that although valproate possesses a weak ability to inhibit HDAC activity, it has many additional targets (Terbach and Williams, 2009).

With regard to the heart, one of the most profound activities of HDAC inhibitors in rodent models is their ability to block fibrosis, which is defined as excess extracellular matrix (ECM) deposition (Schuetze et al., 2014). ECM-rich fibrotic lesions in the heart can cause adverse outcomes, such as fatal arrhythmias and heart failure due to abnormal muscle relaxation and contraction. Pan-, hydroxamate-based HDAC inhibitors have long been recognized for their antifibrotic action in the heart and, more recently, isoform-selective class I HDAC inhibitors were demonstrated to block cardiac fibrosis (Bush and McKinsey, 2010; Nural-Guvener et al., 2014; Williams et al., 2014; Stratton and McKinsey, 2016). Mechanistically, HDAC inhibitors appear to block cardiac fibrosis, in part, by blocking proliferation of cardiac fibroblasts, which are the major ECM-producing cell type in the heart (Williams et al., 2014).

There are currently no FDA-approved therapies for the treatment of cardiac fibrosis; thus, the preclinical findings with HDAC inhibitors in models of cardiac fibrosis have significant clinical implications. Here, we further address the impact of HDAC inhibitors on cardiac fibroblasts, focusing on the hydroxamate pan-HDAC inhibitor trichostatin A (TSA), the benzamide class I HDAC inhibitors, MGCD0103 and MS-275, and the naturally occurring fungal metabolite, apicidin, which is a cyclic peptide class I HDAC-selective inhibitor. Each compound is able to potently block cardiac fibroblast cell cycle progression via induction of antiproliferative gene expression. In contrast, the benzamide HDAC inhibitors elicit changes in fibrosis-related gene expression not observed with TSA and apicidin. This unique activity appears to be due to the ability of the compounds to engage distinct HDAC-containing complexes within cardiac fibroblasts.

Materials and Methods

Primary Adult and Neonatal Cardiac Fibroblast Preparation. Neonatal rat ventricular fibroblasts (NRVFs) were isolated from myocyte preparations from Sprague-Dawley rat pups (postpartum 1 to 2 days), as previously described (Palmer et al., 1995). Adult rat and mouse ventricular fibroblasts (ARVFs and AMVFs, respectively) were collected by the Langendorff-perfusion method from Sprague-Dawley rats and C57Bl/6J mice, respectively (Palmer et al., 1995). NRVFs, ARVFs, and AMVFs were all cultured in Dulbecco's modified Eagle's medium (DMEM) with 20% fetal bovine serum (FBS) containing penicillin (100 U/ml), streptomycin (100 U/ml), and L-glutamine (29.2 μg/ml) (PSG); cells were used at passage 2 for all experiments, unless otherwise stated. Passage "0" cells were treated immediately after isolation at the time of primary culture and harvested 16 hours after isolation/treatment. All cell culture supplies were purchased from Cellgro (Mediatech, Inc., Tewksbury, MA), unless otherwise noted.

HDAC Inhibitors and Agonists. HDAC inhibitors were purchased or synthesized in house and used at the following final concentrations unless otherwise stated: MGCD0103 (1 μM; Selleck Chemicals, Houston, TX), TSA (200–1000 nM; Sigma-Aldrich, St. Louis, MO), apicidin (1–3 μM; Enzo Life Sciences, Farmingdale, New York), and MS-275 (1 μM; Selleck Chemicals). Biaryl-60 (300 nM) and BRD3308 (1 μM) [4-acetamido-*N*-(2-amino-4-fluorophenyl)benzamide] were synthesized in house, and their purity was confirmed to be greater than 95%. Phenylephrine was acquired from Sigma-Aldrich and used at 10 μM, and transforming growth factor (TGF)-β was purchased from Thermo Fisher Scientific (Waltham, MA) and used at a final concentration of 5 ng/ml. For in vivo studies, male C57BL/6 mice were given daily intraperitoneal injections with either vehicle [50:50 dimethylsulfoxide (DMSO)/poly(ethylene glycol) 300] or MGCD0103 at 10 mg/kg, for a total of 3 days.

Mass Spectrometry–Based Quantification of Histone Acetylation. Residue-specific histone acetylation was quantified by the multiplexed mass spectrometry–based method (Kuo et al., 2014). After histones were extracted overnight from the cell pellets using 0.2 N HCl, the extracted histones were treated with propionic anhydride and trypsin digestion, sequentially. The samples of tryptic peptides were then injected into an ACQUITY H-Class ultra-performance liquid chromatography unit (Waters, Milford, MA) coupled to a TSQ Quantum Access triple quadrupole mass spectrometer (Thermo Fisher Scientific) to quantify individual acetylated peptides. The ultra-performance liquid chromatography and tandem mass spectrometry settings, solvent gradient program, and detailed mass transitions were used to detect the elution of the acetylated

peptides as previously reported (Henry et al., 2013; Kuo and Andrews, 2013; Kuo et al., 2014). The resolved peptide peaks were integrated using Xcalibur software (version 2.1; Thermo Fisher Scientific), and the relative quantitative analysis was used to determine the acetylation fraction on individual lysine residues (Liu et al., 2009; Kuo and Andrews, 2013; Kuo et al., 2014).

Immunoblotting and Quantitative Polymerase Chain Reaction. Cell extracts were prepared in radioimmunoprecipitation assay buffer containing Halt Protease and Phosphatase Inhibitor Cocktail (Thermo Fisher Scientific). Protein concentrations were determined using a BCA Protein Assay Kit (Pierce, Rockford, IL). Proteins were resolved by SDS-PAGE, transferred to nitrocellulose membranes (Bio-Rad, Hercules, CA), and probed with antibodies for the following: Ac-H3K4 (NB21-1024; Novus Biologicals, Littleton, CO), Ac-H3K9 (cat. no. NB21-1074; Novus Biologicals), and Ac-H3K18 (cat. no. NB21-1144; Novus Biologicals); Ac-H3K27 (cat. no. ab4729; Abcam, Cambridge, UK) and plasminogen activator inhibitor type 1 (PAI-1) (cat. no. ab28207; Abcam); calnexin (SC-11397; Santa Cruz Biotechnology, Dallas, TX); and phospho-SMAD2/3 (cat. no. 8828; Cell Signaling Technology, Danvers, MA), SMAD2/3 (cat. no. 5678; Cell Signaling Technology), HDAC1 (cat. no. 5356; Cell Signaling Technology), and HDAC2 (cat. no. 5113; Cell Signaling Technology). For total acetyl-lysine immunoblotting, a 1:1 combination of two anti–acetyl-lysine antibodies was used (cat. nos. 9681 and 9441; Cell Signaling Technologies). Horseradish peroxidase–conjugated secondary antibodies (SouthernBiotech, Birmingham, AL) were used at a concentration of 1:2000.

For quantitative polymerase chain reaction (qPCR), total RNA was harvested using TRI Reagent (Life Technologies, Carlsbad, CA). All RNA samples were diluted to 100 ng/μl, and 5 μl (500 ng) was converted to cDNA using the Verso cDNA Synthesis Kit (Thermo Fisher Scientific). qPCR was performed using Absolute QPCR SYBR Green ROX mix (Thermo Fisher Scientific) on a StepOne qPCR instrument (Applied Biosystems, Foster City, CA). Polymerase chain reaction (PCR) primers for p57, urokinase-type plasminogen activator (Plau), matrix metalloprotease Mmp13, PAI-1, and 18S are shown in Supplemental Table 1. All qPCR primers were optimized for a slope between -3.1 and -3.6, >90% efficiency, $R^2 >$ 0.98, and a single melt curve. Relative transcript levels were determined by measuring cycle threshold values using the $\Delta\Delta$ cycle threshold method. For the PCR array, 600 ng pooled RNA (n = 3 plates/group) was processed according to the RT^2 Profiler PCR Array Kit instructions (PAMM-120Z Mouse Fibrosis; QIAGEN, Germantown, MD).

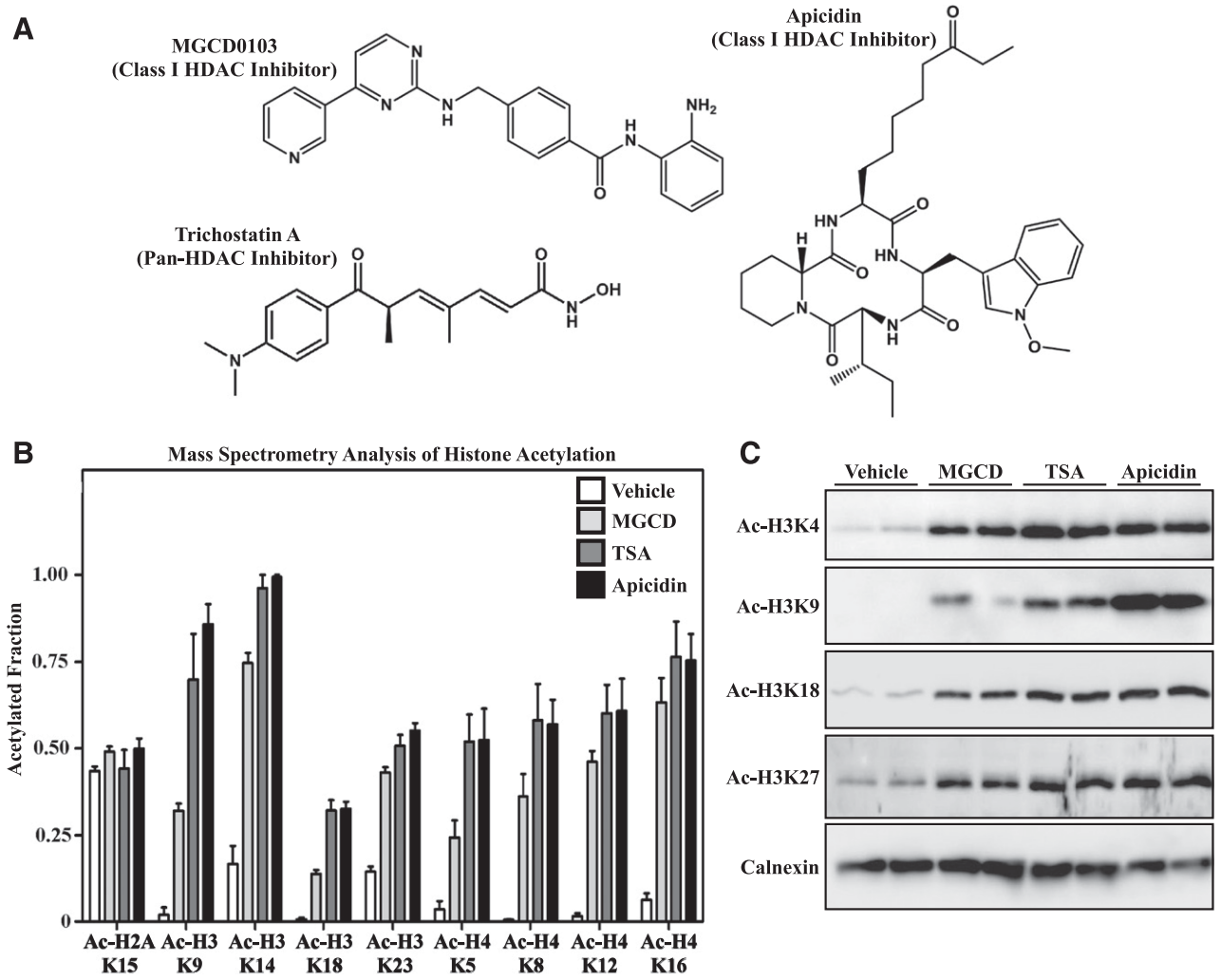

Fig. 1. Effects of structurally distinct HDAC inhibitors on histone acetylation in cardiac fibroblasts. (A) Chemical structures of MGCD0103, TSA, and apicidin. (B) Site-specific changes in acetylation of lysine residues in histones H2A, H3, and H4 were quantified by mass spectrometry using lysates from AMVFs treated with DMSO vehicle control (0.1% final concentration), MGCD0103 (1 μM), TSA (1μM), or apicidin (3 μM) for 24 hours. Data are expressed as the fraction of acetylated versus nonacetylated residues ±S.E.M. (n = 4/group). (C) AMVFs were treated with HDAC inhibitors for 24 hours, homogenized, and subjected to immunoblotting with the indicated anti–acetyl-histone antibodies. Calnexin served as a loading control. Each lane represents an independent plate of cells. MGCD, MGCD0103.

Cell Cycle Analysis. NRVFs were passaged at a 1:6 ratio and cultured for 24 hours in DMEM containing PSG and 20% FBS. Subsequently, cells were cultured in serum starvation medium [DMEM containing 0.1% Nutridoma Supplement (Roche, Indianapolis, IN) and PSG] for 18 hours to synchronize cells in G_0/G_1 of the cell cycle. NRVFs were refed for 32 hours with medium containing 20% FBS in the presence of either vehicle (DMSO) or HDAC inhibitors. Cell cycle analysis was completed by washing NRVFs in cold phosphate-buffered saline (PBS) followed by a 1-minute trypsinization. Cells were washed in PBS and pelleted cells were fixed with ice-cold 70% ethanol. Prior to flow cytometry analysis, samples were placed on ice for 30 minutes and washed once with cold PBS. An equal amount of staining solution (50 μg/ml propidium iodide and 100 μg/ml RNase; Sigma-Aldrich and QIAGEN, respectively) was added to each sample to stain DNA. Samples were processed with a BD FACSCantos II Flow Cytometer (5000 Forward Scatter/Side Scatter [FSC/SSC]-gated cells were captured per sample; BD Biosciences, Franklin Lakes, NJ).

Lentiviral Short-Hairpin RNA Knockdown of HDACs. Lentiviruses were produced with pLKO.1 short hairpin RNA plasmids (Sigma-Aldrich) provided by the University of Colorado Functional Genomics Facility (Aurora, CO), as previously described (Blakeslee et al., 2014). Briefly, on day 1, 2×10^6 human embryonic kidney L293 cells were plated on 10-cm plates in DMEM containing FBS (10%) and PSG. On day 2, each plate was transfected with 9 μg packaging plasmid (psPAX2), 0.9 μg envelope plasmid (pMD2.G), and 9 μg pLKO.1 containing short-hairpin RNA sequence of interest. Plasmids were combined with polyethyleneimine (PEI) at a 3 μl PEI/1 μg DNA mixture; PEI (cat. no. 23966; Polysciences, Inc., Warrington, PA) was used at a concentration of 1 mg/ml. On day 3, the medium was replaced with fresh DMEM containing FBS (10%) and PSG. On day 5, culture medium containing viral particles was filtered and stored at −80°C until use. For infection of cultured fibroblasts in 60-mm plates, 1 ml lentivirus-containing medium was added to 2 ml DMEM, and 3 μl polybrene (10 mg/ml) was included to enhance infection efficiency. Cell homogenates were prepared in radioimmunoprecipitation assay buffer and processed as indicated above. pLKO.1 plasmids were as follows: shControl, SHC016 nonmammalian targeting; shHDAC1, TRCN0000039402; and shHDAC2, TRCN0000039395.

Cellular Thermal Shift Assay. Passage 1 NRVFs were trypsinized, washed, and resuspended in warm PBS at a density of 1×10^6 cells/ml. After thorough mixing, aliquots were made for each treatment group and incubated with DMSO vehicle (0.1% final concentration) or apicidin (3 μM) at 37°C for 3 hours, with rocking, in a cell culture incubator. Cell suspensions were subsequently aliquoted into 12 PCR tubes for each treatment group and subjected to a 12-point temperature gradient (25°C, 44°C, 48°C, 50°C, 52°C, 54°C, 56°C, 58°C, 60°C, 62°C, 64°C, and 68°C) for 3 minutes using a Labnet MultiGene OptiMax thermocycler (Labnet International, Edison, NJ). Immediately after exposure to the temperature gradient, cells were incubated at room temperature for 3 minutes and lysed with three freeze-thaw cycles (dry ice, 25°C water bath). Precipitated proteins and cellular debris were pelleted by centrifugation at 20,000 rcf for 20 minutes at

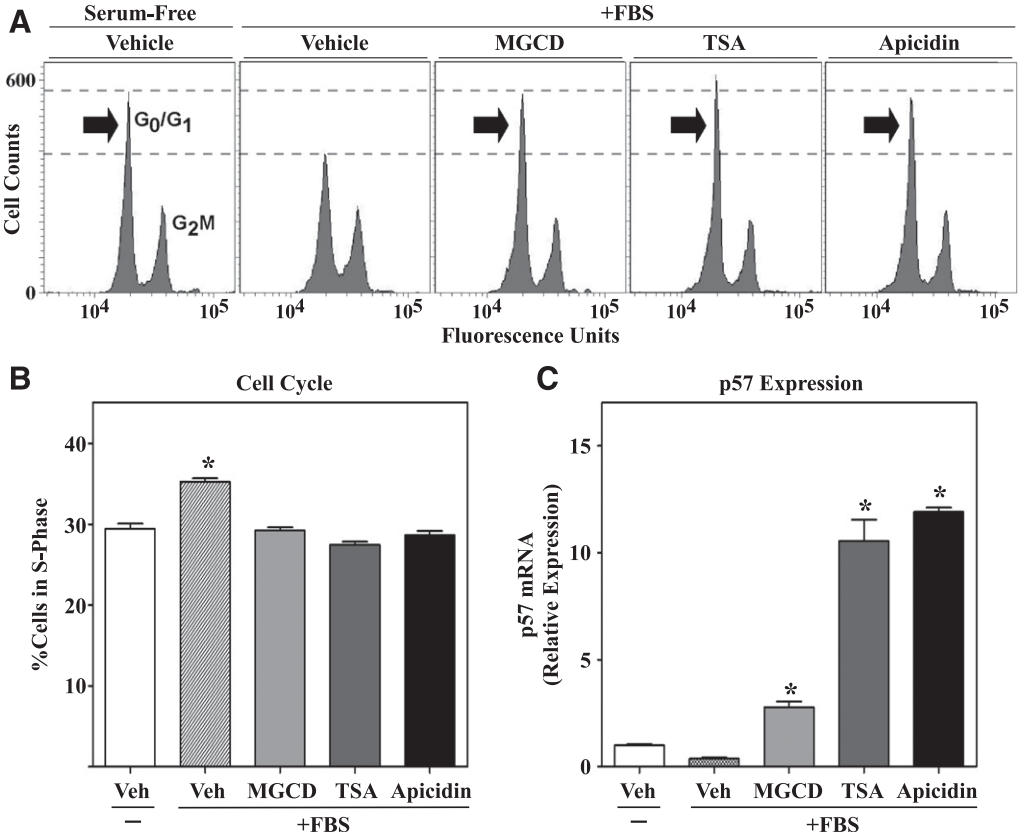

Fig. 2. HDAC inhibitors arrest cardiac fibroblast cell cycle progression via upregulation of p57. Cultured NRVFs were synchronized by serum starvation for 24 hours and subsequently stimulated with FBS (20%) in the absence or presence of DMSO vehicle, MGCD0103 (1 μM), TSA (200 nM), or apicidin (3 μM). At 32 hours after FBS treatment, cells were stained with propidium iodide and cell cycle progression was quantified by flow cytometry. (A) Representative histograms of propidium iodide–stained cells. (B) Quantification of cells in the S phase of the cell cycle (n = 3 plates of cells/condition). Data represent means ± S.E.M. (*$P < 0.05$ versus all other conditions). (C) qRT-PCR was performed with RNA isolated from synchronized ARVFs stimulated for 32 hours in the absence or presence of HDAC inhibitors, as described above. qRT-PCR of p57 was performed with three plates of cells/condition, and technical duplicates were run for each individual sample. Data represent means ± S.E.M. (*$P < 0.05$ versus vehicle-treated cells). MGCD, MGCD0103; qRT-PCR, quantitative reverse transcriptase polymerase chain reaction; Veh, vehicle.

4°C. Supernatants were directly transferred to 4× sample buffer for immunoblot analyses.

Statistical Analysis. Analysis was completed by analysis of variance followed by Tukey post hoc analysis using GraphPad Prism software (GraphPad Inc., La Jolla, CA). Statistical significance ($P < 0.05$) is reported where applicable.

Results

Structurally Distinct HDAC Inhibitors Increase Acetylation of Nucleosomal Histone Tails in Cardiac Fibroblasts. To investigate for potential differential effects of structurally distinct HDAC inhibitors in cardiac fibroblasts, TSA, MGCD0103, and apicidin were employed as representatives of the hydroxamate, benzamide, and cyclic peptide classes, respectively (Fig. 1A). In vitro, TSA is a potent inhibitor of class I and IIb HDACs and is a less effective inhibitor of class IIa catalytic activity (Bradner et al., 2010). In contrast, MGCD0103 and apicidin are highly selective inhibitors of class I HDACs (HDAC1, HDAC2, and HDAC3) (Darkin-Rattray et al., 1996; Fournel et al., 2008; Bradner et al., 2010). Primary AMVFs were serum starved for 18 hours prior to incubation with the indicated HDAC inhibitors for 24 hours. After acid extraction, acetylation of specific lysine residues within the tails of histones H3 and H4 was quantified by mass spectrometry. As shown in Fig. 1B, the three HDAC

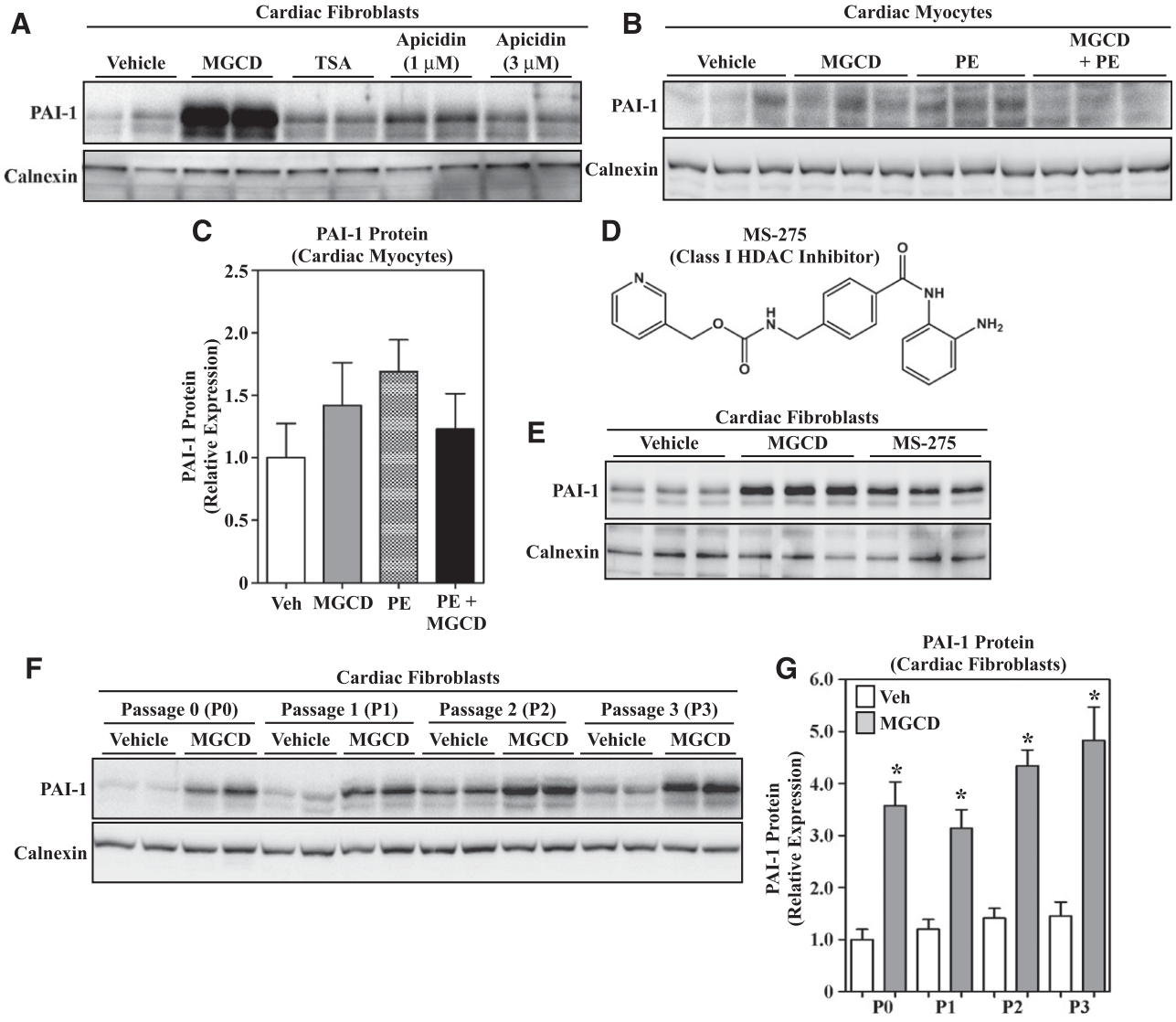

Fig. 3. Benzamide HDAC inhibitors stimulate PAI-1 protein expression in cardiac fibroblasts. (A) Immunoblot analysis of PAI-1 expression in cultured, passage 2 ARVFs treated with DMSO vehicle, MGCD0103 (1 μM), TSA (200 nM), or apicidin (1–3 μM) for 24 hours. (B) Treatment of neonatal rat ventricular cardiomyocytes for 48 hours with MGCD0103 in the absence or presence of the hypertrophic agonist PE (10 μM) failed to enhance PAI-1 expression. (C) The PAI-1 signal in (B) was quantified by densitometry and normalized to the loading control, calnexin. Data represent means ± S.E.M. (differences were not statistically significantly different). (D) Chemical structure of the benzamide class I HDAC inhibitor, MS-275. (E) Treatment of ARVFs with MGCD0103 (1 μM) or MS-275 (1 μM) for 24 hours led to increased PAI-1 protein expression. (F) Passage 0, 1, 2, or 3 ARVFs were treated with MGCD0103 (1 μM) for 16 hours. The ability of MGCD0103 to increase PAI-1 expression was unaffected by myofibroblast phenotype, as defined by the progressive increase in α-smooth muscle actin expression upon fibroblast passage. For all blots, each lane represents an independent plate of cells. (G) The PAI-1 signal in (F), as well as from other samples from an independent preparation of ARVFs (not shown), was quantified by densitometry and normalized to the loading control, calnexin (n = 5 plates of cells/condition). Data represent means ± S.E.M. (*$P < 0.05$ versus vehicle-treated cells). MGCD, MGCD0103; PE, phenylephrine; Veh, vehicle.

inhibitors similarly increased acetylation of multiple lysine residues in both H3 and H4 compared with vehicle treatment but did not affect basal acetylation of histone H2A. These findings were validated by immunoblotting homogenates of HDAC inhibitor–treated AMVFs from an independent experiment using site-specific anti–acetyl-histone antibodies (Fig. 1C).

Structurally Distinct HDAC Inhibitors Block Cardiac Fibroblast Proliferation. In response to stress stimuli, cardiac fibroblasts proliferate and produce excess amounts of ECM. We previously showed that class I HDAC inhibition, with MGCD0103, blocks cardiac fibroblast cell cycle progression in association with upregulation of antiproliferative genes, including the gene encoding the cyclin-dependent kinase inhibitor p57 (Williams et al., 2014); p57 is a potent inhibitor of cell cycle progression (Pateras et al., 2009). To determine whether HDAC inhibition with TSA and apicidin comparably constrains cardiac fibroblast proliferation, NRVFs were synchronized in G_0/G_1 of the cell cycle by serum starvation for 18 hours, and cell cycle progression was reinitiated with FBS in the absence or presence of the HDAC inhibitors for 32 hours. After treatment, cells were fixed and stained with propidium iodide, and flow cytometric analysis was performed to assess cell cycle progression based on cellular DNA content. As shown in Fig. 2A, each of the HDAC inhibitors blocked FBS-induced progression of NRVFs from G_0/G_1 of the cell cycle into the G2/M phase. Quantification of the percentage of NRVFs in the S phase of the cell cycle revealed equivalent antiproliferative effects of the structurally distinct HDAC inhibitors (Fig. 2B). Furthermore, qPCR analysis demonstrated that each HDAC inhibitor potently upregulated mRNA expression of antiproliferative *p57* in ARVFs (Fig. 2C). These cell-based findings suggest that inhibition of cardiac fibroblast proliferation serves as a common mechanism that explains, in part, the ability of TSA, MGCD0103, and apicidin to block cardiac fibrosis in vivo (Kook et al., 2003; Kee et al., 2006; Kong et al., 2006; Gallo et al., 2008; Liu et al., 2008; Nural-Guvener et al., 2014; Williams et al., 2014).

Differential Effects of MGCD0103, TSA, and Apicidin on Expression of PAI-1 in Cardiac Fibroblasts. PAI-1 is a serine protease inhibitor that is known to be involved in the development of pathologic cardiac fibrosis (Ghosh and Vaughan, 2012). During the course of evaluating hearts from mice treated with MGCD0103, a known antifibrotic class I HDAC inhibitor, we noted a modest but paradoxical increase in *PAI-1* mRNA and PAI-1 protein expression in the left ventricles of treated animals (Supplemental Fig. 1) (Nural-Guvener et al., 2014; Williams et al., 2014). Since the heart is composed of multiple cell types, we sought to extend these findings with in vitro analyses employing primary cultured cardiac fibroblasts and myocytes. As shown in Fig. 3A, treatment of ARVFs with MGCD0103, but not TSA or apicidin, led to a marked increase in PAI-1 protein expression. In contrast, MGCD0103 did not alter expression of this serine protease inhibitor in cultured rat cardiac myocytes (Fig. 3, B and C). The related benzamide class I HDAC inhibitor, MS-275, also stimulated PAI-1 protein expression in cultured ARVFs, illustrating a compound class-specific effect on PAI-1 protein expression in cardiac fibroblasts (Fig. 3, D and E). Induction of PAI-1 protein expression by MGCD0103 occurred independently of fibroblast differentiation state, with equivalent increases in PAI-1 observed in low-passage cardiac fibroblasts, as well as in higher-passage cells that are known to express α-smooth muscle actin, indicative of myofibroblast differentiation (Fig. 3, F and G) (Williams et al., 2014). Thus, despite the common ability of benzamide, hydroxamate, and cyclic peptide HDAC inhibitors to increase cardiac fibroblast histone acetylation and block cardiac fibroblast proliferation, only the benzamides exert

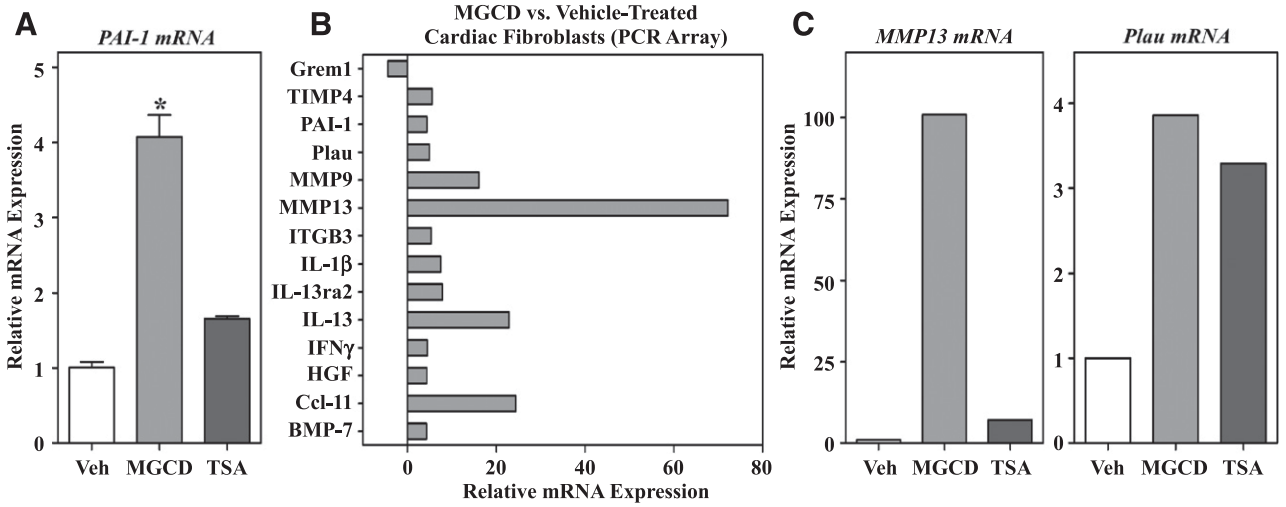

Fig. 4. Differential effects of HDAC inhibitors on fibrosis-related gene expression. (A) qRT-PCR was performed with RNA isolated from cultured AMVFs treated with DMSO vehicle, MGCD0103 (1 μM), or TSA (200 nM) for 24 hours (n = 3 plates of cells/condition with technical duplicates run for each sample). Data represent means ± S.E.M. (*$P < 0.05$ versus all other conditions). (B) RNA was isolated from cultured AMVFs treated with DMSO vehicle or MGCD0103 (1 μM) for 24 hours (n = 3 plates of cells/condition). Pooled cDNA from each group was analyzed for expression of 84 fibrosis-related genes using the QIAGEN RT2 Profiler PCR Array for mouse fibrosis. Shown are the relative changes in mRNA expression between MGCD0103-treated and vehicle-treated cells for all genes that were found to have ≥2-fold change in gene expression. (C) qRT-PCR for MMP13 and Plau was performed with RNA from independent AMVFs to confirm PCR array results. Data shown are target gene expression relative to B2M expression. B2M, β-2 microglobulin; BMP, bone morphogenetic protein; Ccl, CC chemokine ligand; HGF, hepatocyte growth factor; IFN, interferon; IL, interleukin; ITGB, β integrin; MGCD, MGCD0103; qRT-PCR, quantitative reverse transcriptase polymerase chain reaction; TIMP, tissue inhibitor of metalloproteinases; Veh, vehicle.

a paradoxical, robust upregulation of PAI-1 protein expression in this cell type.

Differential Effects of MGCD0103 and TSA on Fibrosis-Related Genes in Cultured Cardiac Fibroblasts. qPCR analysis revealed that MGCD0103, but not TSA, stimulates *PAI-1* mRNA expression (Fig. 4A) in AMVFs, which is consistent with the protein expression data. Because of the dichotomy between PAI-1 expression being generally increased in fibrotic tissue and MGCD0103 treatment being antifibrotic, we sought to determine whether other fibrosis-related genes were differentially expressed after treatment with MGCD0103. AMVFs at passage 2 were treated with either DMSO vehicle or MGCD0103 for 24 hours, and RNA was harvested for PCR array analysis of pro- and antifibrotic genes. Of 84 transcripts in the array, 13 were induced by at least 2-fold with MGCD0103 treatment, and one gene was repressed by the compound (Fig. 4B). Genes that were upregulated by MGCD0103 included *PAI-1* and Plau, the direct protein target of PAI-1. In addition, transcripts for interleukins and MMPs were also upregulated by MGCD0103. To validate these findings and address whether other HDAC inhibitors exerted similar effects on representative fibrosis-related genes, follow-up qPCR studies were performed with RNA from AMVFs treated with either MGCD0103 or TSA. As shown in Fig. 4C, the dramatic induction of *MMP13* mRNA by MGCD0103 that was observed in the PCR array was confirmed by qPCR and, similar to *PAI-1*, was not increased by TSA treatment. In contrast, both MGCD0103 and TSA stimulated *Plau* expression. These findings further illustrate that structurally distinct HDAC inhibitors exert overlapping and divergent effects on cardiac fibroblast gene expression.

Knockdown of HDAC1 or HDAC2 Is Sufficient to Stimulate PAI-1 Expression in Cardiac Fibroblasts. MGCD0103 selectively inhibits HDAC1, HDAC2, and HDAC3. Pharmacologic and genetic approaches were employed to determine whether one of these class I HDACs preferentially regulates PAI-1 protein expression in cardiac fibroblasts, or whether MGCD0103 stimulates PAI-1 expression via an off-target action. Initially, ARVFs were treated with biaryl-60, which is highly selective for HDAC1 and HDAC2 (Moradei et al., 2007; Methot et al., 2008), or BRD3308, which selectively inhibits HDAC3 catalytic activity (Wagner et al., 2016). As shown in Fig. 5, A and B, selective inhibition of HDAC1/2, but not HDAC3, led to increased PAI-1 expression. To extend these findings, expression of HDAC1 and/or HDAC2 was knocked down in AMVFs using lentiviruses encoding short-hairpin RNAs targeting the transcripts for these HDAC isoforms. Reducing expression of either HDAC1 or HDAC2 was sufficient to increase PAI-1 protein levels in AMVFs, and simultaneous

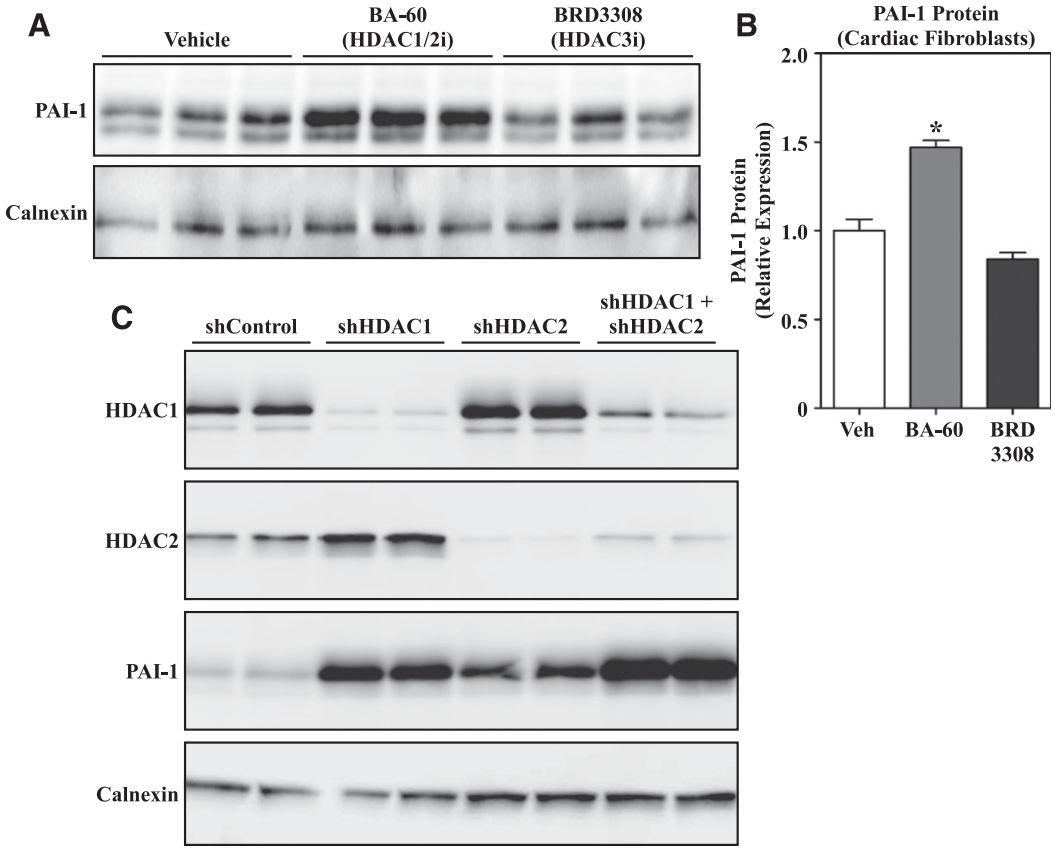

Fig. 5. MGCD0103-induced PAI-1 expression is mediated by HDAC1 and HDAC2 inhibition. (A) Western blot analysis of PAI-1 expression in cultured ARVFs treated with the isoform-selective HDAC inhibitors BA-60 (HDAC1/2 inhibitor, 300 nM) and BRD3308 (HDAC3 inhibitor, 1 μM) for 24 hours. (B) The PAI-1 signal in (A) was quantified by densitometry and normalized to the loading control, calnexin. Data represent means ± S.E.M. (*$P < 0.05$ versus vehicle-treated cells). (C) AMVFs were infected with shControl or lentiviruses encoding shRNAs to target HDAC1 and/or HDAC2. After 96 hours of infection, cell homogenates were subjected to immunoblotting with antibodies specific for HDAC1, HDAC2, and PAI-1. Calnexin served as a loading control. Each lane represents an independent plate of cells. BA-60, biaryl-60; shControl, short-hairpin control lentivirus; shRNA, short-hairpin RNA; Veh, vehicle.

knockdown of both HDAC isoforms led to an additive increase in PAI-1 expression (Fig. 5C). These findings suggest that MGCD0103 stimulates PAI-1 expression in cardiac fibroblasts via targeting HDAC1 and HDAC2, rather than through an off-target mechanism.

MGCD0103-Mediated Induction of PAI-1 Requires De Novo Protein Synthesis. HDAC inhibitors alter gene expression, and they also have diverse nongenomic effects by suppressing HDAC-mediated deacetylation of nonhistone proteins (Choudhary et al., 2009, 2014; Lundby et al., 2012). To address whether MGCD0103 increases PAI-1 protein levels in cardiac fibroblasts via stabilization of existing PAI-1 or through induction of new PAI-1 synthesis, NRVFs were treated with the class I HDAC inhibitor in the absence or presence of cycloheximide (CHX), which blocks de novo protein synthesis. Because of the slow on rate of benzamide HDAC inhibitors (Chou et al., 2008), cells were pretreated with MGCD0103 prior to CHX treatment. As shown in Fig. 6A, MGCD0103-mediated induction of *PAI-1* mRNA expression was retained in the presence of CHX. However, CHX completely blocked MGCD0103-induced PAI-1 protein expression (Fig. 6B). These findings suggest that benzamide HDAC inhibitors elevate PAI-1 protein levels in cardiac fibroblasts through direct stimulation of the gene encoding this serine protease inhibitor, rather than through stabilization of existing PAI-1 protein.

MGCD0103 Does Not Stimulate PAI-1 via Activation of the SMAD Pathway. The canonical pathway for stimulation of the *PAI-1* gene involves TGF-β–mediated phosphorylation of the SMAD transcription factors, resulting in translocation of SMAD to the nucleus and binding of the transcription factor to regulatory elements in the gene encoding *PAI-1* (Nakao et al., 1997). To further address the mechanism by which MGCD0103 enhances PAI-1 expression, experiments were performed to assess the effect of the HDAC inhibitor on the TGF-β/SMAD pathway. ARVFs were treated with MGCD0103 or TGF-β over a time course of 8 hours, and cells were homogenized for immunoblotting with antibodies specific for PAI-1, phosphorylated SMAD2/SMAD3, or total SMAD2/SMAD3. As shown in Fig. 7, MGCD0103 and TGF-β stimulated PAI-1 expression with similar kinetics. However, MGCD0103 failed to stimulate SMAD phosphorylation (Fig. 7A), whereas TGF-β–mediated induction of PAI-1 was coincident with enhanced SMAD phosphorylation (Fig. 7B). These data suggest that MGCD0103-mediated induction of PAI-1 expression occurs independently of the SMAD pathway and is thus not due to stimulation of TGF-β signaling.

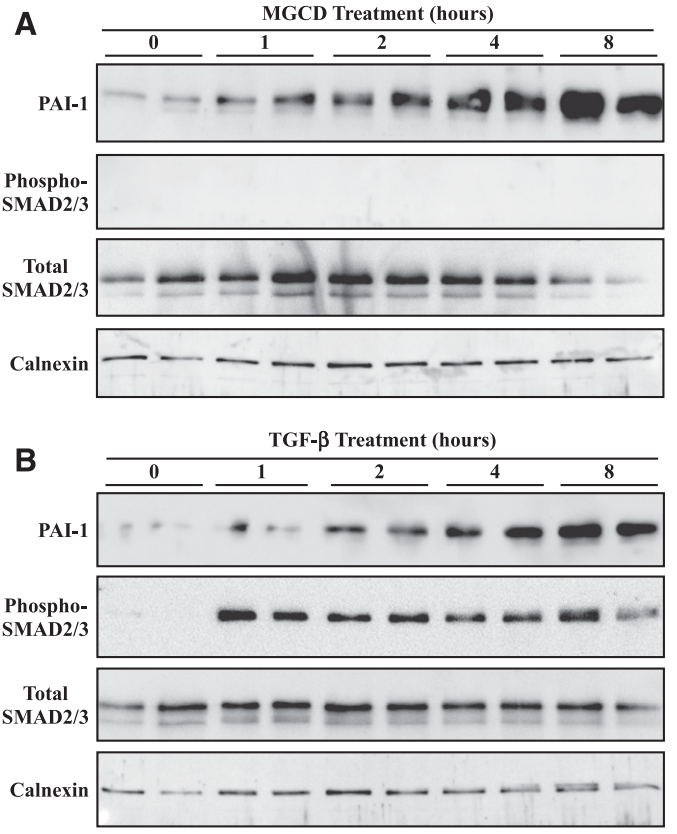

Fig. 7. MGCD0103 does not activate the TGF-β/SMAD pathway. (A and B) ARVFs were treated with 1 μM MGCD0103 (A) or 5 ng/ml TGF-β (B) for the indicated times prior to cell homogenization and immunoblotting with antibodies specific for PAI-1, phospho-SMAD2/3, or total SMAD2/3. Calnexin served as a loading control. Each lane represents an independent plate of cells. MGCD, MGCD0103.

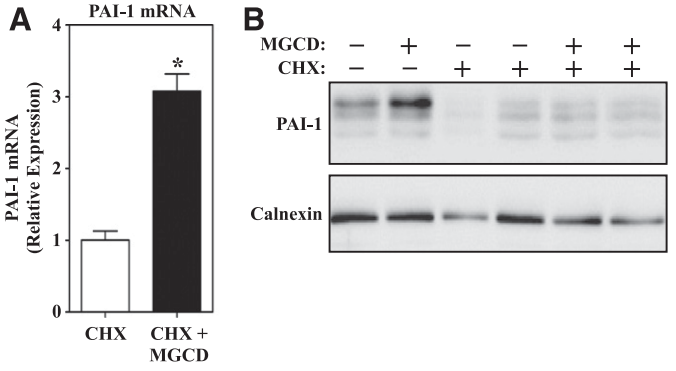

Fig. 6. MGCD0103 promotes de novo synthesis of PAI-1. (A) qRT-PCR was performed with RNA isolated from cultured NRVFs pretreated with either DMSO vehicle or MGCD0103 for 4 hours followed by the addition of CHX at 30 μM for 18 hours (n = 4 plates of cells/condition). Data represent mean PAI-1:18S expression ± S.E.M. (*$P < 0.05$ compared with CHX alone). (B) Immunoblot analysis of PAI-1 expression from ARVFs treated as described above with CHX and MGCD0103. Each lane represents an independent plate of cells. MGCD, MGCD0103; qRT-PCR, quantitative reverse transcriptase polymerase chain reaction.

Structurally Distinct HDAC Inhibitors Differentially Engage HDAC1/2 Complexes in Cardiac Fibroblasts. It is paradoxical that although TSA, MGCD0103, MS-275, and apicidin are all potent inhibitors of HDAC1 and HDAC2, only the benzamides stimulate PAI-1 expression in cardiac fibroblasts. Given the ability of HDAC1/2 knockdown to enhance PAI-1 levels, we considered the possibility that MGCD0103 not only inhibits HDAC catalytic activity but also functionally disrupts HDAC1/2-containing complexes, thereby mimicking knockdown of the proteins. To begin to address this hypothesis, we employed the recently described cellular thermal shift assay (CETSA), which is based on the ability of compounds to thermodynamically stabilize targets to which they are bound (Martinez Molina et al., 2013). NRVFs were treated with DMSO vehicle, MGCD0103, or apicidin, as described in the *Materials and Methods*. Subsequently, the cells were exposed to a heat gradient, followed by centrifugation to pellet denatured proteins that were not bound by MGCD0103 or apicidin. Soluble proteins were then subjected to immunoblotting with antibodies specific

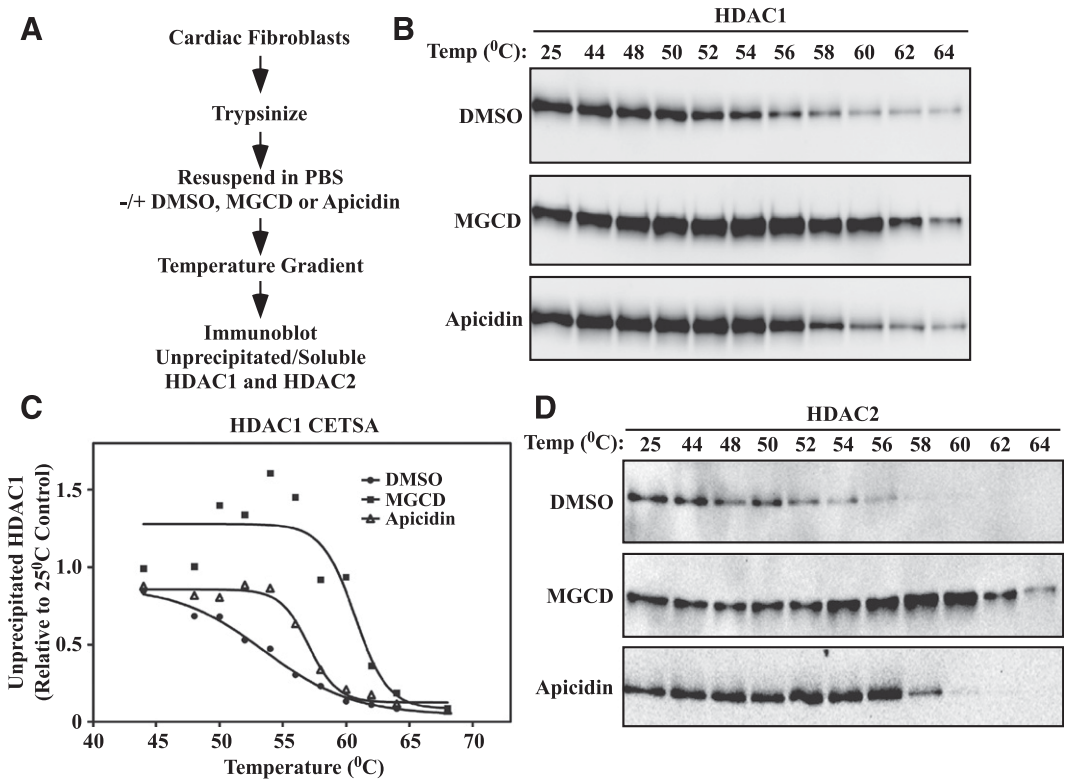

Fig. 8. CETSA suggests differential engagement of HDAC1/2 complexes by MGCD and apicidin. (A) Schematic design of the CETSA protocol. (B) Trypsinized NRVFs were mixed with DMSO vehicle, MGCD0103 (1 μM), or apicidin (3 μM) for 3 hours prior to exposing the mixture to a heat gradient. Soluble, unprecipitated protein was subjected to immunoblotting with an anti-HDAC1 antibody. (C) HDAC1 signal intensity in (B) was quantified by densitometry and plotted relative to the 25°C control. Melting temperatures were calculated using the Boltzman sigmoidal equation for nonlinear fit in GraphPad Prism (DMSO, 53.5°C; MGCD0103, 60.7°C; and apicidin, 57.0°C). (D) The samples shown in (B) were subjected to immunoblotting with an HDAC2-specific antibody. MGCD, MGCD0103.

for HDAC1 or HDAC2 (Fig. 8A). As shown in Fig. 8B, a progressive loss of soluble HDAC1 occurred in a temperature-dependent manner in cardiac fibroblasts treated with DMSO. MGCD0103 provided dramatic heat stabilization of HDAC1, while apicidin was less effective. Consistent with this, upon plotting melting curves, the temperatures at which 50% of HDAC1 was precipitated were determined to be 53.5°C, 60.7°C, and 57.0°C, for DMSO-, MGCD0103-, and apicidin-treated cardiac fibroblasts, respectively (Fig. 8C). MGCD0103 also provided greater heat stabilization to HDAC2 compared with apicidin (Fig. 8D). These findings are consistent with the notion that MGCD0103 and apicidin may differentially bind HDAC1/2-containing complexes in cardiac fibroblasts.

Discussion

This study demonstrates that small molecule HDAC inhibitors from diverse structural classes are able to block proliferation of cardiac fibroblasts in association with enhanced histone acetylation and expression of antiproliferative genes such as *p57*. The findings suggest a generalizable mechanism for suppression of cardiac fibrosis by HDAC inhibitors, whereby the compounds prevent expansion of the pool of ECM-producing fibroblasts in the myocardium in response to stress. Our data also illustrate that despite a common ability of hydroxamate, benzamide, and cyclic peptide HDAC inhibitors to potently suppress the catalytic activity of zinc-dependent HDACs, compounds within these structural classes also trigger distinct transcriptional responses in cardiac fibroblasts. This appears to be due, in part, to differential binding of the compounds to class I HDACs.

TSA, an apicidin derivative, and MGCD0103 have all been shown to block cardiac fibrosis in multiple mouse models (Kook et al., 2003; Kee et al., 2006; Kong et al., 2006; Gallo et al., 2008; Liu et al., 2008; Nural-Guvener et al., 2014; Williams et al., 2014). Furthermore, another benzamide class I HDAC inhibitor, CI-994 [4-acetamido-*N*-(2-aminophenyl)-benzamide], was recently found to reduce cardiac fibrosis in mouse and dog models of heart remodeling (Seki et al., 2016). How can benzamide class I HDAC inhibitors block cardiac fibrosis in vivo, yet stimulate a subset of fibrosis-associated genes in cardiac fibroblasts? We note that the degree of PAI-1 induction in the left ventricles of mice treated with MGCD0103 was extremely modest compared with that observed in cultured cardiac fibroblasts (Supplemental Fig. 1); thus, culturing the cells on high tensile strength plastic, and without neighboring myocytes, may prime the fibroblasts for responsiveness to the class I HDAC inhibitor. Furthermore, the beneficial effect of blocking uncontrolled cardiac fibroblast proliferation with benzamide class I HDAC inhibitors in vivo likely overrides any negative consequences of modest induction of PAI-1 expression or expression of other fibrosis-associated genes in the heart.

Despite the preferential induction of PAI-1 expression in cultured cardiac fibroblasts compared with in the heart in vivo, our findings have important implications for drug

discovery, since even a slight increase in PAI-1 expression could have deleterious long-term consequences. Indeed, given the association of elevated PAI-1 levels with a variety of diseases, including thrombosis, myocardial infarction, and pulmonary dysfunction, inhibitors of PAI-1 are in development (Rouch et al., 2015). It should be noted, however, that *PAI-1* null mice have been shown to develop spontaneous cardiac fibrosis, suggesting the possibility that PAI-1 has cardioprotective actions (Moriwaki et al., 2004; Ghosh et al., 2010, 2013; Xu et al., 2010). Regardless, the knowledge that HDAC1 and HDAC2 have the capacity to directly regulate PAI-1 expression will be important moving forward, as benzamide class I HDAC inhibitors become more widely used in humans (http://www.clinicaltrials.gov). Thus, additional studies should be performed to determine whether HDAC1 and HDAC2 regulate PAI-1 expression in other cell types, such as blood platelets, where PAI-1 is released as a potent antifibrinolytic factor. Furthermore, cell-based assays that monitor PAI-1 expression could be incorporated into HDAC inhibitor drug discovery programs to vet compounds based on this potentially detrimental effect.

In drug development and chemical biology research, it is crucial to establish whether an observed pharmacological effect is due to on- or off-target activity. The ability of benzamide class I HDAC inhibitors to stimulate PAI-1 expression in cardiac fibroblasts appears to be a result of on-target action against HDAC1 and HDAC2, since the stimulatory effect was recapitulated by knocking down these HDACs (Fig. 5B). Based on the CETSA data (Fig. 8), we hypothesize that MGCD0103 functionally mimics HDAC1/2 knockdown by "disrupting" HDAC1/2-containing complexes. CETSA is founded on the ability of compounds to stabilize target proteins and protein complexes, and thereby prevent denaturation of the target(s) upon exposure to a heat gradient (Martinez Molina et al., 2013; Jensen et al., 2015). Our data demonstrate that MGCD0103 is more effective at stabilizing HDAC1 and HDAC2 in cardiac fibroblasts than apicidin. This difference is unlikely related to enzyme inhibition, since apicidin is a more potent inhibitor of HDAC1/2 catalytic activity than MGCD0103, with K_i values of 0.04 and 0.12 nM (apicidin) and 9.0 and 34 nM (MGCD0103) for HDAC1 and HDAC2, respectively (Bradner et al., 2010). Rather, we predict that benzamide HDAC inhibitors alter the structure of HDAC1/2-containing complexes in a manner that leads to heat stabilization and PAI-1 induction.

It is interesting to note that MGCD0103 was generally less effective than TSA and apicidin at stimulating histone acetylation in cardiac fibroblasts (Fig. 1). We cannot rule out the possibility that this difference contributes to induction of PAI-1 or other fibrosis-associated genes by the benzamide HDAC inhibitor.

Our results with PAI-1 are contrary to previously published work. RNA interference–mediated knockdown of *HDAC2* was shown to block TGF-β–induced expression of *PAI-1* in fibroblasts derived from human Peyronie's disease plaques (Ryu et al., 2013), which is converse to the increase in PAI-1 observed upon knockdown of *HDAC2* expression in cardiac fibroblasts (Fig. 5B). Furthermore, butyrate, which is a weak class I HDAC-selective inhibitor (Fass et al., 2010), has been shown to stimulate PAI-1 expression in *v-ras*–transformed rat kidney cells and in rat intestinal epithelial cells (Higgins et al., 1997; Nguyen et al., 2006). However, this stimulatory effect of butyrate was linked to enhanced SMAD phosphorylation and TGF-β signaling (Nguyen et al., 2006), and we failed to observe increased SMAD phosphorylation in cardiac fibroblasts treated with MGCD0103 (Fig. 7A). The discrepancies may be due to differences in fibroblast origin (heart versus penile plaques for the HDAC2 studies), as well as induction of SMAD phosphorylation via off-target actions of butyrate, such as by inducing the endoplasmic reticulum stress pathway (Zhang et al., 2016).

In conclusion, TSA, MGCD0103, and apicidin are three structurally distinct HDAC inhibitors that exert antifibrotic effects in preclinical models of cardiac fibrosis (Schuetze et al., 2014; Stratton and McKinsey, 2016). Despite this similarity, however, we have shown that these compounds have distinctly divergent effects on fibrosis-related gene expression in isolated primary cardiac fibroblasts, which is likely due to the manner in which they engage protein complexes harboring HDAC1 and HDAC2 catalytic units. These findings have important implications for HDAC inhibitor drug development and highlight the need to employ multiple, structurally distinct compounds when applying a chemical biology approach to assess HDAC isoform function.

Acknowledgments

The authors thank Bradley S. Ferguson and Frederick A. Schroeder for technical support and critical discussions.

Authorship Contributions

Participated in research design: Schuetze, Stratton, McKinsey.

Conducted experiments: Schuetze, Stratton, Blakeslee, Kuo.

Contributed new reagents or analytic tools: Wempe, Wagner, Holson, Kuo, Andrews, Gilbert, Hooker.

Performed data analysis: Schuetze, Stratton, McKinsey.

Wrote or contributed to the writing of the manuscript: Schuetze, Stratton, McKinsey.

References

Bantscheff M, Hopf C, Savitski MM, Dittmann A, Grandi P, Michon AM, Schlegl J, Abraham Y, Becher I, Bergamini G, et al. (2011) Chemoproteomics profiling of HDAC inhibitors reveals selective targeting of HDAC complexes. *Nat Biotechnol* **29**:255–265.

Blakeslee WW, Wysoczynski CL, Fritz KS, Nyborg JK, Churchill ME, and McKinsey TA (2014) Class I HDAC inhibition stimulates cardiac protein SUMOylation through a post-translational mechanism. *Cell Signal* **26**:2912–2920.

Bradner JE, West N, Grachan ML, Greenberg EF, Haggarty SJ, Warnow T, and Mazitschek R (2010) Chemical phylogenetics of histone deacetylases. *Nat Chem Biol* **6**:238–243.

Bush EW and McKinsey TA (2010) Protein acetylation in the cardiorenal axis: the promise of histone deacetylase inhibitors. *Circ Res* **106**:272–284.

Chou CJ, Herman D, and Gottesfeld JM (2008) Pimelic diphenylamide 106 is a slow, tight-binding inhibitor of class I histone deacetylases. *J Biol Chem* **283**: 35402–35409.

Choudhary C, Kumar C, Gnad F, Nielsen ML, Rehman M, Walther TC, Olsen JV, and Mann M (2009) Lysine acetylation targets protein complexes and co-regulates major cellular functions. *Science* **325**:834–840.

Choudhary C, Weinert BT, Nishida Y, Verdin E, and Mann M (2014) The growing landscape of lysine acetylation links metabolism and cell signalling. *Nat Rev Mol Cell Biol* **15**:536–550.

Darkin-Rattray SJ, Gurnett AM, Myers RW, Dulski PM, Crumley TM, Allocco JJ, Cannova C, Meinke PT, Colletti SL, Bednarek MA, et al. (1996) Apicidin: a novel antiprotozoal agent that inhibits parasite histone deacetylase. *Proc Natl Acad Sci USA* **93**:13143–13147.

Fass DM, Shah R, Ghosh B, Hennig K, Norton S, Zhao WN, Reis SA, Klein PS, Mazitschek R, Maglathlin RL, et al. (2010) Effect of inhibiting histone deacetylase with short-chain carboxylic acids and their hydroxamic acid analogs on vertebrate development and neuronal chromatin. *ACS Med Chem Lett* **2**:39–42.

Fenichel MP (2015) FDA approves new agent for multiple myeloma. *J Natl Cancer Inst* **107**:djv165.

Finnin MS, Donigian JR, Cohen A, Richon VM, Rifkind RA, Marks PA, Breslow R, and Pavletich NP (1999) Structures of a histone deacetylase homologue bound to the TSA and SAHA inhibitors. *Nature* **401**:188–193.

Fournel M, Bonfils C, Hou Y, Yan PT, Trachy-Bourget MC, Kalita A, Liu J, Lu AH, Zhou NZ, Robert MF, et al. (2008) MGCD0103, a novel isotype-selective histone deacetylase inhibitor, has broad spectrum antitumor activity in vitro and in vivo. *Mol Cancer Ther* **7**:759–768.

Gallo P, Latronico MV, Gallo P, Grimaldi S, Borgia F, Todaro M, Jones P, Gallinari P, De Francesco R, Ciliberto G, et al. (2008) Inhibition of class I histone deacetylase with an apicidin derivative prevents cardiac hypertrophy and failure. *Cardiovasc Res* **80**:416–424.

Ghosh AK, Bradham WS, Gleaves LA, De Taeye B, Murphy SB, Covington JW, and Vaughan DE (2010) Genetic deficiency of plasminogen activator inhibitor-1 promotes cardiac fibrosis in aged mice: involvement of constitutive transforming growth factor-beta signaling and endothelial-to-mesenchymal transition. *Circulation* **122**:1200–1209.

Ghosh AK, Murphy SB, Kishore R, and Vaughan DE (2013) Global gene expression profiling in PAI-1 knockout murine heart and kidney: molecular basis of cardiac-selective fibrosis. *PLoS One* **8**:e63825.

Ghosh AK and Vaughan DE (2012) PAI-1 in tissue fibrosis. *J Cell Physiol* **227**: 493–507.

Gregoretti IV, Lee YM, and Goodson HV (2004) Molecular evolution of the histone deacetylase family: functional implications of phylogenetic analysis. *J Mol Biol* **338**:17–31.

Henry RA, Kuo YM, and Andrews AJ (2013) Differences in specificity and selectivity between CBP and p300 acetylation of histone H3 and H3/H4. *Biochemistry* **52**: 5746–5759.

Higgins PJ, Ryan MP, and Jelley DM (1997) P52PAI-1 gene expression in butyrate-induced flat revertants of v-ras-transformed rat kidney cells: mechanism of induction and involvement in the morphological response. *Biochem J* **321**:431–437.

Jensen AJ, Martinez Molina D, and Lundbäck T (2015) CETSA: a target engagement assay with potential to transform drug discovery. *Future Med Chem* **7**:975–978.

Kee HJ, Sohn IS, Nam KI, Park JE, Qian YR, Yin Z, Ahn Y, Jeong MH, Bang YJ, Kim N, et al. (2006) Inhibition of histone deacetylation blocks cardiac hypertrophy induced by angiotensin II infusion and aortic banding. *Circulation* **113**:51–59.

Kong Y, Tannous P, Lu G, Berenji K, Rothermel BA, Olson EN, and Hill JA (2006) Suppression of class I and II histone deacetylases blunts pressure-overload cardiac hypertrophy. *Circulation* **113**:2579–2588.

Kook H, Lepore JJ, Gitler AD, Lu MM, Wing-Man Yung W, Mackay J, Zhou R, Ferrari V, Gruber P, and Epstein JA (2003) Cardiac hypertrophy and histone deacetylase-dependent transcriptional repression mediated by the atypical homeodomain protein Hop. *J Clin Invest* **112**:863–871.

Kuo YM and Andrews AJ (2013) Quantitating the specificity and selectivity of Gcn5-mediated acetylation of histone H3. *PLoS One* **8**:e54896.

Kuo YM, Henry RA, and Andrews AJ (2014) A quantitative multiplexed mass spectrometry assay for studying the kinetic of residue-specific histone acetylation. *Methods* **70**:127–133.

Liu B, Lin Y, Darwanto A, Song X, Xu G, and Zhang K (2009) Identification and characterization of propionylation at histone H3 lysine 23 in mammalian cells. *J Biol Chem* **284**:32288–32295.

Liu F, Levin MD, Petrenko NB, Lu MM, Wang T, Yuan LJ, Stout AL, Epstein JA, and Patel VV (2008) Histone-deacetylase inhibition reverses atrial arrhythmia inducibility and fibrosis in cardiac hypertrophy independent of angiotensin. *J Mol Cell Cardiol* **45**:715–723.

Lundby A, Lage K, Weinert BT, Bekker-Jensen DB, Secher A, Skovgaard T, Kelstrup CD, Dmytriyev A, Choudhary C, Lundby C, et al. (2012) Proteomic analysis of lysine acetylation sites in rat tissues reveals organ specificity and subcellular patterns. *Cell Reports* **2**:419–431.

Martinez Molina D, Jafari R, Ignatushchenko M, Seki T, Larsson EA, Dan C, Sreekumar L, Cao Y, and Nordlund P (2013) Monitoring drug target engagement in cells and tissues using the cellular thermal shift assay. *Science* **341**:84–87.

McKinsey TA (2012) Therapeutic potential for HDAC inhibitors in the heart. *Annu Rev Pharmacol Toxicol* **52**:303–319.

Methot JL, Chakravarty PK, Chenard M, Close J, Cruz JC, Dahlberg WK, Fleming J, Hamblett CL, Hamill JE, Harrington P, et al. (2008) Exploration of the internal cavity of histone deacetylase (HDAC) with selective HDAC1/HDAC2 inhibitors (SHI-1:2). *Bioorg Med Chem Lett* **18**:973–978.

Moradei OM, Mallais TC, Frechette S, Paquin I, Tessier PE, Leit SM, Fournel M, Bonfils C, Trachy-Bourget MC, Liu J, et al. (2007) Novel aminophenyl benzamide-type histone deacetylase inhibitors with enhanced potency and selectivity. *J Med Chem* **50**:5543–5546.

Moriwaki H, Stempien-Otero A, Kremen M, Cozen AE, and Dichek DA (2004) Overexpression of urokinase by macrophages or deficiency of plasminogen activator inhibitor type 1 causes cardiac fibrosis in mice. *Circ Res* **95**:637–644.

Mottamal M, Zheng S, Huang TL, and Wang G (2015) Histone deacetylase inhibitors in clinical studies as templates for new anticancer agents. *Molecules* **20**: 3898–3941.

Nakao A, Imamura T, Souchelnytskyi S, Kawabata M, Ishisaki A, Oeda E, Tamaki K, Hanai J, Heldin CH, Miyazono K, et al. (1997) TGF-beta receptor-mediated signalling through Smad2, Smad3 and Smad4. *EMBO J* **16**:5353–5362.

Nguyen KA, Cao Y, Chen JR, Townsend CM, Jr, and Ko TC (2006) Dietary fiber enhances a tumor suppressor signaling pathway in the gut. *Ann Surg* **243**: 619–625, discussion 625–627.

Nural-Guvener HF, Zakharova L, Nimlos J, Popovic S, Mastroeni D, and Gaballa MA (2014) HDAC class I inhibitor, mocetinostat, reverses cardiac fibrosis in heart failure and diminishes CD90+ cardiac myofibroblast activation. *Fibrogenesis Tissue Repair* **7**:10.

Palmer JN, Hartogensis WE, Patten M, Fortuin FD, and Long CS (1995) Interleukin-1 beta induces cardiac myocyte growth but inhibits cardiac fibroblast proliferation in culture. *J Clin Invest* **95**:2555–2564.

Pateras IS, Apostolopoulou K, Niforou K, Kotsinas A, and Gorgoulis VG (2009) p57KIP2: "Kip"ing the cell under control. *Mol Cancer Res* **7**:1902–1919.

Rouch A, Vanucci-Bacqué C, Bedos-Belval F, and Baltas M (2015) Small molecules inhibitors of plasminogen activator inhibitor-1 - an overview. *Eur J Med Chem* **92**: 619–636.

Ryu JK, Kim WJ, Choi MJ, Park JM, Song KM, Kwon MH, Das ND, Kwon KD, Batbold D, Yin GN, et al. (2013) Inhibition of histone deacetylase 2 mitigates profibrotic TGF-β1 responses in fibroblasts derived from Peyronie's plaque. *Asian J Androl* **15**:640–645.

Schuetze KB, McKinsey TA, and Long CS (2014) Targeting cardiac fibroblasts to treat fibrosis of the heart: focus on HDACs. *J Mol Cell Cardiol* **70**:100–107.

Seki M, LaCanna R, Powers JC, Vrakas C, Liu F, Berretta R, Chacko G, Holten J, Jadiya P, Wang T, et al. (2016) Class I histone deacetylase inhibition for the treatment of sustained atrial fibrillation. *J Pharmacol Exp Ther* **358**:441–449.

Stratton MS and McKinsey TA (2016) Epigenetic regulation of cardiac fibrosis. *J Mol Cell Cardiol* **92**:206–213.

Terbach N and Williams RS (2009) Structure-function studies for the panacea, valproic acid. *Biochem Soc Trans* **37**:1126–1132.

Wagner FF, Lundh M, Kaya T, McCarren P, Zhang YL, Chattopadhyay S, Gale JP, Galbo T, Fisher SL, Meier BC, et al. (2016) An isochemogenic set of inhibitors to define the therapeutic potential of histone deacetylases in β-cell protection. *ACS Chem Biol* **11**:363–374.

Wagner FF, Weïwer M, Lewis MC, and Holson EB (2013) Small molecule inhibitors of zinc-dependent histone deacetylases. *Neurotherapeutics* **10**:589–604.

Wagner JM, Hackanson B, Lübbert M, and Jung M (2010) Histone deacetylase (HDAC) inhibitors in recent clinical trials for cancer therapy. *Clin Epigenetics* **1**: 117–136.

Williams SM, Golden-Mason L, Ferguson BS, Schuetze KB, Cavasin MA, Demos-Davies K, Yeager ME, Stenmark KR, and McKinsey TA (2014) Class I HDACs regulate angiotensin II-dependent cardiac fibrosis via fibroblasts and circulating fibrocytes. *J Mol Cell Cardiol* **67**:112–125.

Xu Z, Castellino FJ, and Ploplis VA (2010) Plasminogen activator inhibitor-1 (PAI-1) is cardioprotective in mice by maintaining microvascular integrity and cardiac architecture. *Blood* **115**:2038–2047.

Zhang J, Yi M, Zha L, Chen S, Li Z, Li C, Gong M, Deng H, Chu X, Chen J, et al. (2016) Sodium butyrate induces endoplasmic reticulum stress and autophagy in colorectal cells: implications for apoptosis. *PLoS One* **11**:e0147218.

Address correspondence to: Timothy A. McKinsey, Division of Cardiology and Consortium for Fibrosis Research and Translation, Department of Medicine, University of Colorado Anschutz Medical Campus, 12700 E. 19th Avenue, RC2 8450, Aurora, CO 80045. E-mail: timothy.mckinsey@ucdenver.edu